치의과학박사 학위논문

EVALUATION OF THE ACCURACY OF DENTAL MODELS FABRICATED BY VARIOUS 3D PRINTERS

다양한 3D 프린터로 제작한 치과 모형의 정확도 평가

2018 년 2 월

서울대학교 대학원

치의과학과 치과 보철과 전공

전 진

ABSTRACT

EVALUATION OF THE ACCURACY OF DENTAL MODELS FABRICATED BY VARIOUS 3D PRINTERS

Jin Jeon, D.D.S., M.S.

Department of Prosthodontics,
Graduate School, Seoul National University
(*Directed by Professor* **Seong-Joo Heo**, D.D.S., M.S.D., Ph.D.)

Objectives. Optical impressions obtained with an intraoral scanner and prosthesis fabrication using computer-aided design (CAD)/computer-aided manufacturing (CAD) were introduced into the field of dentistry in the early 1980s. With the recent development and increasing popularity of intraoral scanners, direct digital acquisition of the dental arch in the mouth has become more readily available, omitting the step of conventional impression acquisition. In some simple cases, physical models are not required with digital impressions; however, physical dental models are mandatory in many extensive cases. Rapid prototyping or 3D printing can be used to fabricate models from digital impression data. The purpose of this study was to evaluate the dimensional accuracy and reproducibility of compartments in full arch models made with various 3D printing methods including digital light processing (DLP), fused deposition modeling (FDM), stereolithography (SLP) and photopolymer jetting (Polyjet).

Material and Methods. The mandibular model was modified to generate reference CAD data in reverse engineering software. To simulate an implant scan body, 6 cylinders were placed in the left and right canines (#33, #43), second premolars (#35, #45) and second molars (#37, #47). The cylinders in the left (#37) and right second molars (#47) were designed to have mesial and distal angulation of 30° to simulate off-axis implant angulations. Three additional reference spheres were placed around the left second molar (#37) to set coordinates for deviations. Ten models were printed with 4 different printers and 5 materials using the CAD data file. The printed models were scanned with a model scanner and merged with the original CAD data. Difference color maps were used to evaluate deviations and surface textures were examined with photographs and scanning electron microscopy. The systemic mean deviations of models from each 3D printer were

analyzed in a superimposition study. Deviations at different cylinder locations in the X-, Y-, and Z-axes, and total linear deviations were analyzed in a coordinate study.

Results. In the superimposition study, FDM yielded the highest mean deviations with statistical significance ($p < 0.05$). There were no significant differences among the other printer groups. In the coordinate study, FDM and DLP showed the most positive deviations in the left second molar position in the X-axis; the mean deviations gradually decreased as the position shifted rightward. In contrast, SLA and Polyjet showed the most negative deviations in the left second molar position in the X-axis and values gradually increased as the position shifted rightward. In the Y-axis, FDM exhibited forward deviations on the right side and DLP showed backward deviations in the anterior site and forward deviations in the posterior site. In the Z-axis, all printers showed little deviation in canine and premolar regions, with maximum deviation in second molar sites. The total linear deviation was lowest in the left canine region and deviations increased with distance from this site in all groups.

Conclusion. FDM showed more systemic deviations than DLP, Polyjet and SLA in the superimposition study, but all printed models were within a clinically acceptable range. Bucco-lingually, FDM and DLP showed expansion while Polyjet and SLA showed contraction. Anterior-posteriorly, FDM generally showed forward deviations and DLP showed forward deviations in the molar region and backward deviations in the anterior region. In the vertical dimension, there were no significant deviations in the anterior region but significant deviations were found in the molar region. For all printers, total linear deviations were lowest in the anterior region and became larger as the position moved backwards.

Key words: 3-dimensional printing; accuracy; additive manufacturing; dental model; rapid prototyping.

Student Number: 2013-31204

CONTENTS

I. INTRODUCTION

Optical impression acquisition with intraoral scanners and prosthesis fabrication using computer-aided design (CAD)/computer-aided manufacturing (CAM) has evolved significantly since its introduction to the field of dentistry in the 1980s. With the recent development and increasing popularity of intraoral scanners, direct digital acquisition of the dental arch in the mouth has become more widely used than ever before.[1-3] In this context, CAD/CAM is used to produce dental restorations using digital data.[4] The CAM process is divided into 2 categories: subtractive manufacturing such as milling processes and additive manufacturing, also known as rapid prototyping or 3-dimensional (3D) printing.[5] Referred to as the fourth industrial revolution, 3D printing technology has undergone rapid evolution and application in medicine makes up to 20% of overall usage.

When only digital impressions are obtained with an intraoral scanner, prostheses are generated in the absence of physical models. Yet, accurate replicates of the dental arch are often required to provide information about inner fit, proximal contact and occlusal form used to generate the prosthesis via CAD/CAM. Physical models are mandatory for complex extended prostheses such as complete or partial dentures, when extra porcelain build-up is needed and information about the adjacent and occluding teeth is critical. Models can be generated from intraoral scanning data through either milling or 3D printing.

As per the ISO 5725-1 definition[6], the general term “accuracy” can be used to describe both trueness and precision. Trueness refers to how closely the test result resembles the reference while precision addresses how closely repeated test results resemble one another. Poor model trueness can give rise to problems such as longer durations of chair-side prosthesis adjustment and subsequently patient discomfort and compromised longevity of the prosthesis.[7-9] Additionally, if the accuracy of a model made with intraoral scan data using 3D printing is insufficient compared to

a stone model made from conventional impression, the effectiveness of the digital treatment might be questioned. There are few studies concerning the accuracy of casts produced by intraoral digital impression.[10-12]

There are a number of 3D printers of different schemes available on the market today. Stereolithography (SLA) printers have high accuracy, offer good resolution and yield smoother surface finishes compared to other printing methods.[13-15] Yet, a majority of studies investigating 3D printer characteristics come from the fields of biomechanics and engineering and rarely involve dental applications.[16] There are few studies regarding the 3D accuracy of dental models made by rapid prototyping and specifically of full arch models made by 3D printing. Additionally, it is difficult to find guidelines about suitable material properties, appropriate 3D printer types, and optimal fabrication conditions for dental models. The size, shape and surface of teeth as well as the relationships between opposing and adjacent teeth vary patient-to-patient. Thus, there is a need to evaluate the clinical validity of various 3D printers, printing materials and model qualities in a dentistry context. Specifically, there is need for a comparative assessment of volumetric differences and quantitative deviations among full arch models made with 3D printers.

The purpose of this study was to evaluate the dimensional accuracy and reproducibility of compartments in full arch models made with various 3D printing methods including digital light processing (DLP), fused deposition modeling (FDM), SLA and Photopolymer jetting (Polyjet). Overall dimensional changes across full arch models were assessed in a superimposition study and 3D deviations of specific landmarks were analyzed in a coordinate study. The null hypothesis was that the reproducibility of full arch models made with 3D printers was poor (i.e., not accurate).

II. MATERIALS AND METHODS

CAD design and manufacturing

In order to simulate a situation in which implant scan bodies were connected to a lower dental arch for implant restoration, a lower dental model (Prosthetic Restoration Jaw Model, Nissin Dental Products Inc., Kyoto, Japan) was scanned and modified in reverse engineering software (Rapidform 2004; Inus Technology Inc., Seoul, Korea). Six cylinders were placed in the left and right canines (#33, #43), second premolars (#35, #45) and second molars (#37, #47). The cylinders in the left and right second molars were designed to have mesial and distal angulation of 30° to simulate off-axis implant angulation. Three additional reference spheres were placed around the left second molar (#37) to set coordinates for deviations (Fig. 1).

Model fabrication from 3D printers

Four 3D printers with different printing schemes were compared in this study: FDM (Creator Pro; Flashforge, Zhejiang, China), DLP (D1-150; Veltz3D, Incheon, Korea), Polyjet (Eden 260V; Stratasys, Eden Prairie, Minnesota, USA) and SLA (Form 2; Formlabs, Somerville, Massachusetts, USA). For the DLP (D1-150) printer, 2 different resins were used: DM-1 (Aekyung Chemical Co., Ltd., Seoul, Korea) and Model (NextDent, Soesterberg, Netherlands), and are identified as DLP 1 and DLP 2, respectively. Thus, there were a total of 5 experimental groups in this study (Table 1). Ten models were printed for each group from original CAD data in accordance with manufacturer instructions.

FDM printers build objects by heating and extruding thermoplastic filaments. The extrusion nozzles move along the X-, Y-, and Z-axes, constructing layer-by-layer in accordance with the dimensions of an object. The layer thickness of the Creator Pro printer is 100–500 μm and was set to 100 μm in this study.

SLA printers also build structures layer-by-layer similar to FDM, but use a photo-curable photopolymer rather than thermoplastic filament, typically a liquid resin that hardens after focused light or ultraviolet exposure. In this study, the laser spot size was set to 145 μm with power of 250 mW. The layer thickness of the Form 2 printer was 50 μm. Printed models were cleaned in 95% ethanol for 20 min and post-curing was performed in a UV curing unit for 60 min as per the manufacturer instructions. The slice angle was set to 120° for Form 2 only based on manufacturer recommendations.

Like SLA printers, DLP printers use liquid resin-based photopolymers but instead cure entire slices using a digital light projector. The D1-150 had an XY resolution of 78 μm and a Z resolution of 25 μm.

Polyjet is a printing technology that jets layers of liquid photopolymer using a special head and subsequently cures the materials using ultraviolet light. In this study, the layer thickness of the Polyjet printer was set to 16 μm.

To evaluate the accuracy of 3D-printed models, all models were scanned with a desktop model scanner (Identica T500, Medit, Seoul, Korea) with an accuracy of 7 μm (ISO 12836[17]). The surfaces of models made using the D1-150, Eden 260V and Form 2 printers were lightly dusted with powder (3D Laser Scanning Spray; Helling GmbH, Heidgraben, Germany) to reduce light reflection before scanning.

Data analysis by image merging and coordinate studies

To evaluate the accuracy of 3D-printed models, the original CAD data and the scanned data of experimental models were imported into Geomagic Verify 3D analysis software (3D systems, Morrisville, North Carolina, USA). Superimposition and coordinate studies were performed by a single well-educated operator. The 3D models consisted of more than 60,000 points and each model was arranged and superimposed using a best fit algorithm in which every point in the model was as close as possible to corresponding points in the CAD data.

Differences between the superimposed images were calculated and the mean values were drawn. Difference color maps were generated to show differences between the experimental and reference models and the degree of distortion in the full arch.

To evaluate linear distortions on the X-, Y-, and Z-axes, the scanned data of printed models were aligned along a reference plane and the differences of cylinder top centers were calculated. The origin was set as the center of the sphere located on the buccal side of the left lower second molar. And the X-Y plane was defined as a plane that contained the centers of the 3 spheres. The Y-axis was defined as a line that passed through the origin parallel to the line containing the centers of the other spheres in the X-Y plane. The X-axis was defined as a line that passed through the origin perpendicular to the Y-axis in the X-Y plane. Finally, the Z-axis was defined as a line that passed through the origin perpendicular to the X-Y plane (Fig. 5). The X, Y, Z coordinates of the cylinder top centers (#37i, #35i, #33i, #43i, #45i, #47i) were measured. A positive X-value indicated that the center of the cylinder was farther and a negative X-value indicated that it was closer. A positive Y-value indicated that the center point was deviated forward and a negative Y-value indicated that it deviated backwards. A positive Z-value indicated that the center point deviated upwards and a negative Z-value indicated that it deviated downwards. The following formula was used to calculate the linear distances of centers between the experimental and reference CAD data.

$$d = \sqrt{(s_x - m_x)^2 + (s_y - m_y)^2 + (s_z - m_z)^2}$$

Statistical analysis

The data were analyzed with the IBM SPSS ver. 20.0 statistical software package. In the superimposition study, a 1-way ANOVA was used to compare differences in polygons between the CAD model and experimental models. In the coordinate study, a 2-way ANOVA was used to test differences in the X-, Y-, and Z-axes and

in the linear distances of the centers of cylinder tops. *Post hoc* Tukey tests were used for pairwise comparisons. The significance level was set at $\alpha = 0.05$.

III. RESULTS

Superimposition study

The mean systematic deviations of 3D printers measured by differences in polygons between experimental models and the reference model are shown in Table 2. FDM group showed the highest mean deviation among the experimental groups (160.0 ± 10.0 μm, $p < 0.05$). DLP 1, DLP 2, Polyjet and SLA groups showed systemic deviations of 94.7 ± 20.2 μm, 105.2 ± 8.0 μm, 105.5 ± 25.4 μm and 120.3 ± 37.5 μm, respectively. There were no significant differences among the other 4 groups (Table 2 and Fig. 6).

Difference color map

The deviation patterns of printed models were visually assessed using difference color maps. FDM models showed a relatively wide range of deviations and prominent striations. Models printed with DLP 1 and DLP 2 had minimal deviations in anterior regions and contractions in molar regions. Models printed with Polyjet and SLA generally showed minimal distortions (Fig. 7).

Coordinate study

Mean differences in the X-, Y-, and Z-coordinates of the 6 cylinder centers among 3D-printed models are shown in Table 3 and Fig. 8. There were significant differences among 3D printers in all 3 axes. In the X-axis, FDM (−61.3 μm), DLP 1 (−22.5 μm) and DLP 2 (−18.8 μm) groups showed negative mean deviations while Polyjet (34.3 μm) and SLA (44.4 μm) groups showed positive mean deviations. In the Y-axis, FDM (109.5 μm), DLP 1 (21.9 μm) and Polyjet (20.1 μm) groups

showed positive mean deviations, while DLP 2 (−14.8 μm) and SLA (−34.0 μm) groups showed negative mean deviations. In the Z-axis, FDM (34.0 μm) group showed positive deviations and Polyjet (−21.4 μm) group showed negative deviations, and the other 3 groups showed relatively minor deviations < 8 μm.

Deviations in the X-, Y-, and Z-axes at different cylinder locations are shown in Table 4 and Fig. 9–11 and were significantly different ($p < 0.05$) in all axes. In the X-axis, FDM, DLP 1 and DLP 2 groups showed the most positive values in the left second molar position (#37i), and the mean value gradually decreased as the position moved rightward along the arch. In contrast, for Polyjet and SLA groups, the most negative value appeared in the left second molar (#37i) and the mean increased as the position moved to rightward.

In the Y-axis, FDM group had positive values except at the #37i position and deviations increased as the position moved farther rightward from the center. DLP 1 and DLP 2 groups showed negative values in the front side and positive values in the molar region. Polyjet group generally showed positive values except at the #47i position. SLA group showed the lowest value in the left second molar (#37i) position among the 5 experimental groups.

There were only minor deviations observed in the Z-axis, amounting to < 2 μm in the canine and premolar regions with the largest deviations at second molar sites (#37i, #47i). FDM and SLA groups showed positive deviations at #37i while DLP 1, DLP 2 and Polyjet groups showed negative deviations at this position. In the #47i position, FDM, DLP 1 and DLP 2 groups showed positive deviations while Polyjet and SLA groups showed negative deviations.

Total linear deviations were calculated at different cylinder locations (Table 5 and Fig. 12). The smallest deviations were detected at the #33i position and the largest deviations were detected at the #47i position in all groups. Positions farther from the #33i position showed increasing deviation sizes except for #35i, which showed larger deviations than #37i in FDM models.

Surface texture

In FDM models, interlayer connections were rough and had prominent demarcation lines. There were some parts that appeared “molten,” especially the tops of cylinders and pointy parts like cusp tips. In DLP 1 and DLP 2 models, staircases between layers were apparent and in some models, it seemed that sharp tips had been chipped out. Surfaces of Polyjet models were the smoothest and had the most gloss but lacked sharpness on cylinder tops. In SLA models, hatched interlayer connections were relatively smooth and the surface showed some degree of gloss.

The tops of cylinders and cusp tips on the first premolar were evaluated using a scanning electron microscope (SEM) with a magnification ratio of 30. The FDM models showed distinguishable stepped layers of printed filament materials with round margins. DLP 1 and DLP 2 models showed marked interlayer configurations and rather jagged edges. Polyjet models had no distinguishable interlayer lines but were relatively dull in line angles and points. SLA models showed detectable interlayer lines but contours were smooth (Fig. 13 and 14).

IV. DISCUSSION

In this study, we analyzed the accuracy of models printed with 4 different 3D printers using 5 different materials. In the superimposition study, FDM group showed significantly larger deviations than the other 4 groups. Additionally, FDM models had rougher surfaces in photographs and on SEM. In additive manufacturing, layer-by-layer printing can yield a staircase effect on the printed surface. This effect is most prominent with the use of thick layering materials, resulting in a rougher surface and more dimensional errors. A main reason for issues with FDM models in this study might have been that the nozzle was raised

substantially (100 μm) for each layer.

In the coordinate study, the mean deviations of all 6 cylinders were analyzed in the X-, Y-, and Z-axes for each group. In the X-axis, FDM, DLP 1 and DLP 2 groups showed contraction while Polyjet and SLA groups showed expansion bucco-lingually in a statistically significant manner. In the Y-axis, FDM, DLP 1 and Polyjet groups deviated anteriorly while DLP 2 and SLA groups deviated posteriorly. In the Z-axis, FDM group deviated upwards and Polyjet group deviated downwards, while the other 3 groups only showed minor deviations (< 8 μm). FDM group showed the largest deviations in all axes.

Deviations in the X-, Y-, and Z-axes were also analyzed at 6 different cylinder locations. In the X-axis, FDM, DLP 1 and DLP 2 groups showed the highest values in the left second molar (#37i) and this value decreased as the position moved rightward along the arch. In contrast, Polyjet and SLA groups showed the lowest values in the left second molar (#37i) and values increased as the position moved rightward. This indicated that FDM, DLP 1 and DLP 2 groups were generally contracted to the midline of the arch while Polyjet and SLA groups were expanded in the buccal direction, given that the origin point was an absolute 0 point.

In the Y-axis, FDM group showed backward deviations in the #37i position and forward deviations in other positions, with the largest deviations observed as the position moved rightward from the center. DLP 1 and DLP 2 groups showed backward deviations in the canines and forward deviations in the molars so that the models seemed contracted towards the center of the arch. Polyjet group generally exhibited forward deviations with the exception of backward deviations at the #47i position. SLA group showed the largest backward deviations at the #37i position and deviation decreased as the position moved anteriorly.

X and Y deviations were supposed to share the same properties because the contour of the X-Y table is simultaneously determined as a layer and layers are stacked along the Z-axis. In the Z-axis, deviations were generally smaller than those

in the X- and Y-axes and deviations < 3 μm was observed in canine and premolar regions. In terms of vertical accuracy, significant deviations were observed in molar but not anterior regions. A 30° tilt in the #37i and #47i cylinders may have affected vertical accuracy in the molar region. When the vertical dimension of models is not accurate, the prosthesis might show a higher occlusal dimension or might not occlude with counterpart teeth. If occlusion of the prosthesis is too low, a remake is typically necessary. Alternatively, if occlusion is too high, patients are subjected to prolonged chair-side adjustment times and extensive adjustment can result in lower masticatory efficiency and compromise the lifespan of the prosthesis.

Total linear deviations at the 6 cylinder positions were also assessed. The smallest deviations were detected in #33i. Increasing distance from #33i was associated with larger deviations with the exception that, in the FDM model, there were larger deviations at #35i than at #37i. Position #47i (the farthest position from #33i) showed the largest deviations for all printers. Position 40-series cylinders on the right side also showed larger deviations compared to the same positions on the left, although this difference was not always statistically significant. And this might have been due to the relatively longer distances from the origin point.

Stone models have long been used as the gold standard for diagnosis, treatment planning and prosthetic fabrication in dentistry[18]; however, stone models have several disadvantages as they are prone to fracture and degradation and require a dedicated space for storage.[19] To overcome these disadvantages, digital models acquired from intraoral scanners have been proposed as a virtual alternative to stone models.[20] Yet, physical models are still required in some cases of extended prosthetic treatment. In the early stages of development, models from CAD/CAM were only made by subtractive methods such as block or disc milling. Schmitz et al.[21] reported that the dimensional accuracy of subtractive manufacturing can be compromised by thermal expansion or contraction of the machine structure and cutting tools, vibration while machining, and wearing and bending of the burs.

Additionally, tip size of milling bur and rotating ability of the machine can limit the detail and shape of models made by subtractive milling.

Rapid prototyping or 3D printing has several advantages over subtractive manufacturing for making casts from digital data. The scheme of additive manufacturing is that 3D design data is cross-sectioned into many thin layers and a printing machine stacks printing materials based on the geometric data for each layer. Additive manufacturing can produce complex models with undercuts and cavities that are otherwise difficult or impossible to make.[22, 23] Three-dimensional printing is increasingly used in the field of dentistry to make diagnostic models for orthodontic or prosthetic treatment planning, surgical guides for implants, framework for extensive prosthesis, wax patterns for casting, complete dentures, and oromaxillofacial prostheses.

SLA, invented by Charles Hull[24], makes models by polymerizing layers of a light-curable resin. A focused ultraviolet (UV) laser beam draws contours of a model onto the surface of a liquid photopolymer, curing a thin layer. Then, the polymerized surface is dipped to a fixed level into the liquid bath, allowing the object to rewet with fresh liquid. In this manner, the laser beam polymerizes new layers on top of the previous layer in a stepwise fashion to form a 3D model.[24, 25] After printing, the model is removed from the bath and post-cured in a UV cabinet.[26]

FDM builds models in a layer-by-layer fashion similar to SLA, but a main difference is that the layering materials are solid thermoplastic filaments. The 3D model is built up by extruding heated thermoplastics onto a bed along a path guided by the model data. Once a layer has been placed, the nozzle is raised by a fixed interval and the next layer is printed on the top of the previous layer. This process is repeated to build the model.[26] Supporting structures are also required for FDM models because it takes time for the layers to fuse together and for the material to harden.[27] In this study, printed material used for FDM was polylactic acid, which has lower melting point (150~160°C) than acrylonitrile butadiene styrene.

The Polyjet modeling method is performed by jetting liquid photopolymer to build layers as thin as 16 μm (the setting used in this study). After jetting, each layer is immediately cured by UV light so that fully printed models can be used immediately without additional post-curing. To maintain complicated geometries, a gel-like support made from separate material is used and is readily detached by hand or by water jetting.[26] Of note, Polyjet modeling is more time consuming and expensive than other methods.

DLP and SLA printers share many features in common. The basic scheme and printer design are the same and in both cases the materials are photopolymers that require light curing. A main difference is that DLP uses a digital light projector for curing so that each layer is solidified all at once and not drawn out by a laser as in SLA. For this reason, DLP is generally faster than other printers. The accuracy of DLP printing depends largely on the projector resolution.

Model accuracy can be influenced by several factors such as manufacturing conditions, material type, printing layer thickness, degree of polymerization shrinkage, and the size and strength of the curing unit. Shrinkage in the amount of 6–10% can occur during photopolymerization and have an effect on overall accuracy.[28] Thermal expansion or contraction during the curing process can also result in dimensional errors.[29-31] Laser overcuring due to the size of tip and extended exposure between each layer may be an important source of dimensional and positional errors, especially in the vertical direction.[25] Postcuring processes of additional polymerization using UV light and heat can also cause model warping. Finally, detaching force applied to separate models from the printing platform before the completion of curing might cause deformation. In this study, total linear deviations were more prominent in the molar region than in the anterior region; this might have been due to the relative distances of these regions from the center of the object. When a uniform object deforms, the absolute amount of deformation increases as the distance between measuring points increases.

Alharbi et al.[16] evaluated the accuracy of single crowns that were printed with SLA method at different slice angles. Accuracy was highest at a 120° slice angle where supporting rods were minimal. In this study, a 120° slice angle was only applied for SLA models as recommended by the manufacturer.

Even though the stone model is a gold standard, it has its own issues with deformation and up to 0.3% expansion allowed by American Dental Association specifications. Hazeveld et al.[32] argued that measurement differences of less than 0.25 mm are acceptable for clinical practice because the tolerances for manual measurements are almost identical to that value. Another study by Bell at al.[33] concerning the accuracy of digital models argued that a mean difference of 0.27 mm would not have significant clinical effects. Moreover, Hirogaki et al.[34] mentioned that a measurement difference of 0.30 mm could be considered accurate enough for study models in orthodontics.

Keating et al.[35] compared the accuracy of traditional plaster maxillary models, digital virtual models and replica models made by rapid prototyping. Replica models showed significant differences in the vertical dimension (Z-plane) compared to the other 2 groups and this might be due to the use of a relatively thick layer (0.15 mm) of clear resin material. Thus, it was concluded that additive rapid prototyping models were not adequate for clinical use given low accuracy and surface detail, while 3D virtual models had comparatively higher accuracy and anatomical details.

Alternatively, Cuperus et al.[36] utilized a real maxillary skull to acquire digital models with an intraoral scanner and generate replica models with the stereolithographic method. A comparison revealed that although replica models were significantly less accurate than digital models, they were within the acceptable range for clinical use.

A comparative study of the accuracy of dental replica models made with FDM and SLA was conducted by Kasparova et al.[37] In this study, models made with SLA

showed more accuracy and better surface detailing than those made with FDM. Nevertheless, FDM and SLA models did not show significant differences with conventional stone models, so it was concluded that 3D-printed models were a suitable replacement for stone models. Lee et al.[38] scanned natural molar teeth with a desktop scanner and printed with FDM and Polyjet printers in order to conduct a 3D analysis with the superimposition method. In this study, the FDM method was significantly less accurate than the Polyjet method, but both were within the clinically acceptable range. Hazeveld et al.[32] reported mean systematic deviations of −0.02 mm, 0.04 mm, and 0.25 mm for the Polyjet, DLP and 3D printing (3DP) models, respectively. Although the 3DP model showed significantly higher mean differences, the authors concluded that all 3 printing methods were sufficiently accurate and reproducible for clinical use. Murugesan et al.[39] assessed surface anatomical details and the dimensional accuracy of unilateral mandibular models made with FDM, Polyjet and 3DP, and reported that the Polyjet method was the most accurate, followed by 3DP and FDM. In microscopic images, the surface details of Polyjet models showed definitive cusps and developmental grooves as well as a smooth surface fiber pattern.

In this study, overall mean deviations of test printers were less than 250 μm, indicating that the models were clinically acceptable; however, it should be considered that deviations were larger in distal regions than in anterior regions.

At present, there are several types of 3D printers on the market that offer a wide range of printing options. In a clinical context, practical factors should be considered such as printer cost, printer volume and weight, printing speed, build dimension, available material properties, heat and noise management, convenience of modeling software, ease of setup, use and maintenance in addition to accuracy.

V. CONCLUSIONS

Within the limitations of this study, FDM group exhibited more systemic deviations than DLP, Polyjet and SLA models in a superimposition study, but all printed models demonstrated accuracy within a clinically acceptable range. FDM and DLP models showed bucco-lingual expansion while Polyjet and SLA models showed bucco-lingual contraction. Anterior-posteriorly, FDM models showed generally forward deviations and DLP models showed backward deviations in the anterior region and forward deviations in the molar region. In the vertical dimension, there were no significant deviations in the anterior region but significant deviations existed in the molar region. Total deviations were the lowest in the canine position and became larger as the position moved backwards for all printers.

References

1. Lee SJ, Gallucci GO. Digital vs. conventional implant impressions: efficiency outcomes. Clin Oral Implants Res 2013; 24: 111-115.
2. Miyazaki T, Hotta Y, Kunii J, Kuriyama S, Tamaki Y. A review of dental CAD/CAM: current status and future perspectives from 20 years of experience. Dent Mater J 2009; 28: 44-56.
3. Davidowitz G, Kotick PG. The use of CAD/CAM in dentistry. Dent Clin North Am 2011; 55: 559-570.
4. Beuer F, Schweiger J, Edelhoff D. Digital dentistry: an overview of recent developments for CAD/CAM generated restorations. Br Dent J 2008; 204: 505-511.
5. Alharbi N, Osman R, Wismeijer D. Effects of build direction on the mechanical properties of 3D-printed complete coverage interim dental restorations. J Prosthet Dent 2016; 115: 760-767.
6. ISO 5725-1:1994 Accuracy (trueness and precision) of measurement methods and results — Part 1: General principles and definitions.
7. Persson AS, Oden A, Andersson M, Sandborgh-Englund G. Digitization of simulated clinical dental impressions: virtual three-dimensional analysis of exactness. Dent Mater 2009; 25: 929-936.
8. Perakis N, Belser UC, Magne P. Final impressions: a review of material properties and description of a current technique. Int J Periodontics Restorative Dent 2004; 24: 109-117.
9. Wettstein F, Sailer I, Roos M, Hammerle CH. Clinical study of the internal gaps of zirconia and metal frameworks for fixed partial dentures. Eur J Oral Sci 2008; 116: 272-279.
10. Kim SY, Kim MJ, Han JS, Yeo IS, Lim YJ, Kwon HB. Accuracy of dies captured by an intraoral digital impression system using parallel confocal imaging. Int J Prosthodont 2013; 26: 161-163.
11. Guth JF, Keul C, Stimmelmayr M, Beuer F, Edelhoff D. Accuracy of digital models obtained by direct and indirect data capturing. Clin Oral Investig 2013; 17: 1201-1208.
12. Flugge TV, Schlager S, Nelson K, Nahles S, Metzger MC. Precision of intraoral digital dental impressions with iTero and extraoral digitization with the iTero and a model scanner. Am J Orthod Dentofacial Orthop 2013; 144: 471-478.
13. Melchels FP, Feijen J, Grijpma DW. A review on stereolithography and its applications in biomedical engineering. Biomaterials 2010; 31: 6121-6130.
14. Abduo J, Lyons K, Bennamoun M. Trends in computer-aided manufacturing in prosthodontics: a review of the available streams. Int J Dent 2014; 2014: 783948.

15. van Noort R. The future of dental devices is digital. Dent Mater 2012; 28: 3-12.
16. Alharbi N, Osman RB, Wismeijer D. Factors influencing the dimensional accuracy of 3D-printed full-Coverage dental restorations using stereolithography technology. Int J Prosthodont 2016; 29: 503-510.
17. ISO 12836:2015 Dentistry - Digitizing devices for CAD/CAM systems for indirect dental restorations - Test methods for assessing accuracy.
18. Bell A, Ayoub AF, Siebert P. Assessment of the accuracy of a three-dimensional imaging system for archiving dental study models. J Orthod 2003; 30: 219-223.
19. White AJ, Fallis DW, Vandewalle KS. Analysis of intra-arch and interarch measurements from digital models with 2 impression materials and a modeling process based on cone-beam computed tomography. Am J Orthod Dentofacial Orthop 2010; 137: 451-459.
20. Ender A, Attin T, Mehl A. In vivo precision of conventional and digital methods of obtaining complete-arch dental impressions. J Prosthet Dent 2016; 115: 313-320.
21. Schmitz TL, Ziegert JC, Canning JS, Zapata R. Case study: a comparison of error sources in high-speed milling. Precis Eng 2008; 32: 126-133.
22. Vojdani M, Torabi K, Farjood E, Khaledi A. Comparison the marginal and internal fit of metal copings cast from wax patterns fabricated by CAD/CAM and conventional wax up techniques. J Dent (Shiraz) 2013; 14: 118-129.
23. Torabi K, Farjood E, Hamedani S. Rapid prototyping technologies and their applications in prosthodontics, a review of literature. J Dent (Shiraz) 2015; 16: 1-9.
24. Hull CW. Apparatus for production of three-dimensional objects by stereolithography. US Patent 4,575,330, March 11, 1986.
25. Pham DT, Ji C. Design for stereolithography. Proceedings of the institution of mechanical engineers, Part C: J Mech End Sci 2000; 214: 635-640.
26. Olszewski R, Reychler H. Clinical applications of rapid prototyping models in cranio-maxillofacial surgery. Advanced applications of rapid prototyping technology in modern engineering. InTech; 2011: 173–206
27. Ohtani T, Kusumoto N, Wakabayashi K, Yamada S, Nakamura T, Kumazawa Y, Yatani H, Sohmura T. Application of haptic device to implant dentistry - Accuracy verification of drilling into a pig bone. Dent Mater J 2009; 28: 75-81.
28. Gabriel B, Miguel C, Guillermo L, Eugenio O. Numerical analysis of stereolithography processes using the finite element method. Rapid Prototyping J 1995; 1: 13-23.
29. Hong W, Lee YT, Gong H. Thermal analysis of layer formation in a stepless

rapid prototyping process. Appl Therm Eng 2004; 24: 255-268.
30. Hong W, Lee Yong T, Gong H. A study of the staircase effect induced by material shrinkage in rapid prototyping. Rapid Prototyping J 2005; 11: 82-89.
31. O'Brien DJ, Mather PT, White SR. Viscoelastic properties of an epoxy resin during cure. J Compos Mater 2001; 35: 883-904.
32. Hazeveld A, Huddleston Slater JJR, Ren Y. Accuracy and reproducibility of dental replica models reconstructed by different rapid prototyping techniques. Am J Orthod Dendofac 2014; 145: 108-115.
33. Bell A, Ayoub AF, Siebert P. Assessment of the accuracy of a three-dimensional imaging system for archiving dental study models. J Orthod 2003; 30: 219-223.
34. Hirogaki Y, Sohmura T, Satoh H, Takahashi J, Takada K. Complete 3-D reconstruction of dental cast shape using perceptual grouping. IEEE Trans Med Imaging 2001; 20: 1093-1101.
35. Keating AP, Knox J, Bibb R, Zhurov AI. A comparison of plaster, digital and reconstructed study model accuracy. J Orthod 2008; 35: 191-201.
36. Cuperus AM, Harms MC, Rangel FA, Bronkhorst EM, Schols JG, Breuning KH. Dental models made with an intraoral scanner: a validation study. Am J Orthod Dentofacial Orthop 2012; 142: 308-313.
37. Kasparova M, Grafova L, Dvorak P, Dostalova T, Prochazka A, Eliasova H, Prusa J, Kakawand S. Possibility of reconstruction of dental plaster cast from 3D digital study models. Biomed Eng Online 2013; 12: 49.
38. Lee KY, Cho JW, Chang NY, Chae JM, Kang KH, Kim SC, Cho JH. Accuracy of three-dimensional printing for manufacturing replica teeth. Korean J Orthod 2015; 45: 217-225.
39. Murugesan K, Anandapandian PA, Sharma SK, Vasantha Kumar M. Comparative evaluation of dimension and surface detail accuracy of models produced by three different rapid prototype techniques. J Indian Prosthodont Soc 2012; 12: 16-20.

Figure Legends

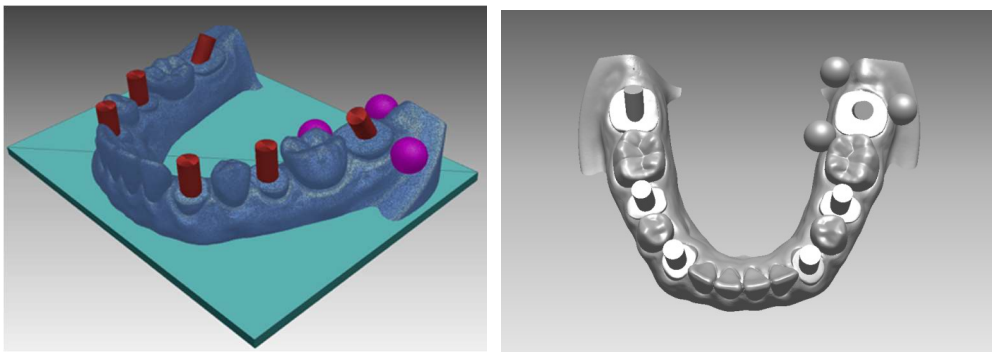

a b

Fig. 1 Six cylinders were placed in the left and right canines (#33, #43), second premolars (#35, #45), and second molars (#37, #47). Three additional reference spheres were placed around the left second molar (#37) to set coordinates for deviations.

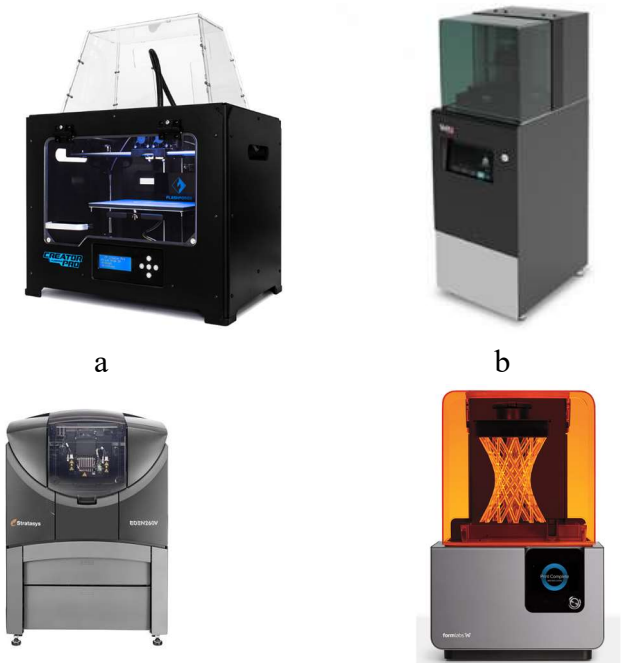

a b c d

Fig. 2 FDM (Creator Pro) (a), DLP (D1-150) (b), Polyjet (Eden 260V) (c) and SLA (Form 2) (d) use different technologies for 3D printing.

a. FDM (Creator Pro)

b. DLP 1 (D1-150-DM)

c. DLP 2 (D1-150-ND)

d. Polyjet (Eden 260V)

e. SLA (Form 2)

Fig. 3 Models from each group, FDM (Creator Pro) (a), DLP 1 (D1-150-DM) (b), DLP 2 (D1-150-ND) (c), Polyjet (Eden 260V) (d) and SLA (Form 2) (e).

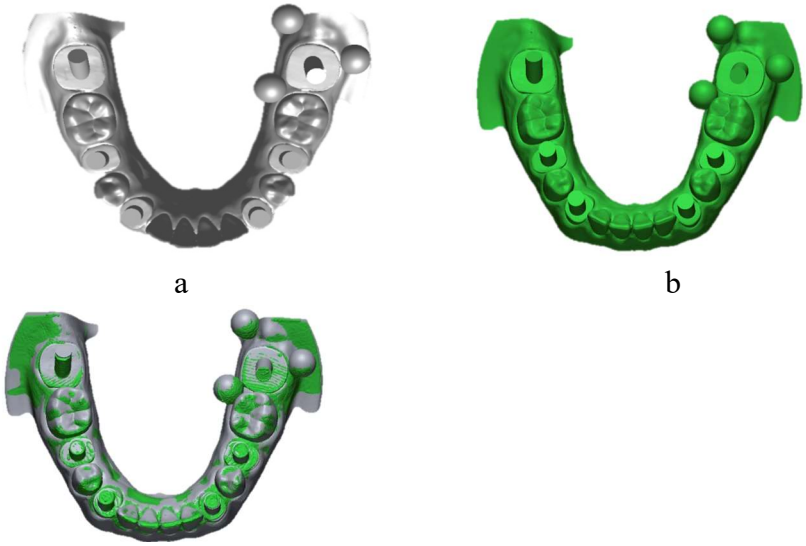

Fig. 4 The original CAD data (a) and scanned experimental models (b) were merged with best fit algorithm (c) and the deviations were calculated and analyzed.

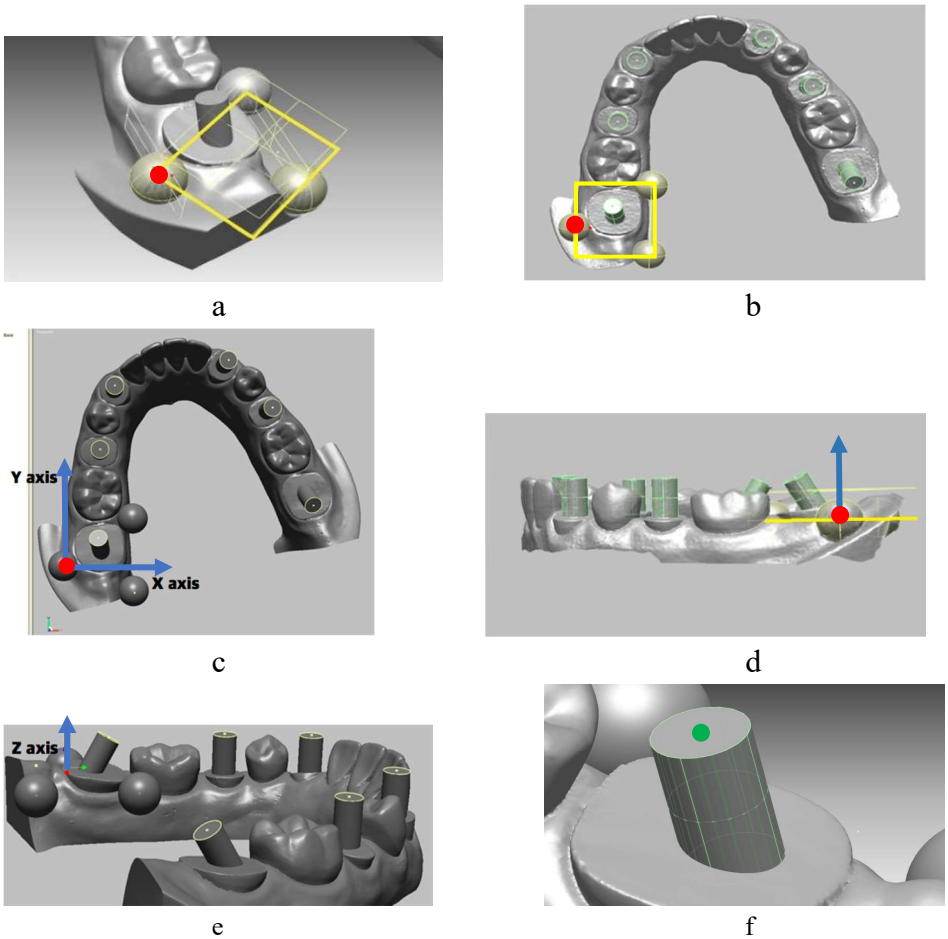

Fig. 5 . The origin (red dot) was set as the center of the sphere located on the buccal side of the left lower second molar (a). And the X-Y plane (yellow square) was defined as a plane that contained the centers of the 3 spheres (b). The Y-axis was defined as a line that passed through the origin parallel to the line containing the centers of the other spheres in the X-Y plane. The X-axis was defined as a line that passed through the origin perpendicular to the Y-axis in the X-Y plane (c and d). Finally, the Z-axis was defined as a line that passed through the origin perpendicular to the X-Y plane (d and e). The X, Y, Z coordinates of the cylinder top centers (green dot) were measured (f).

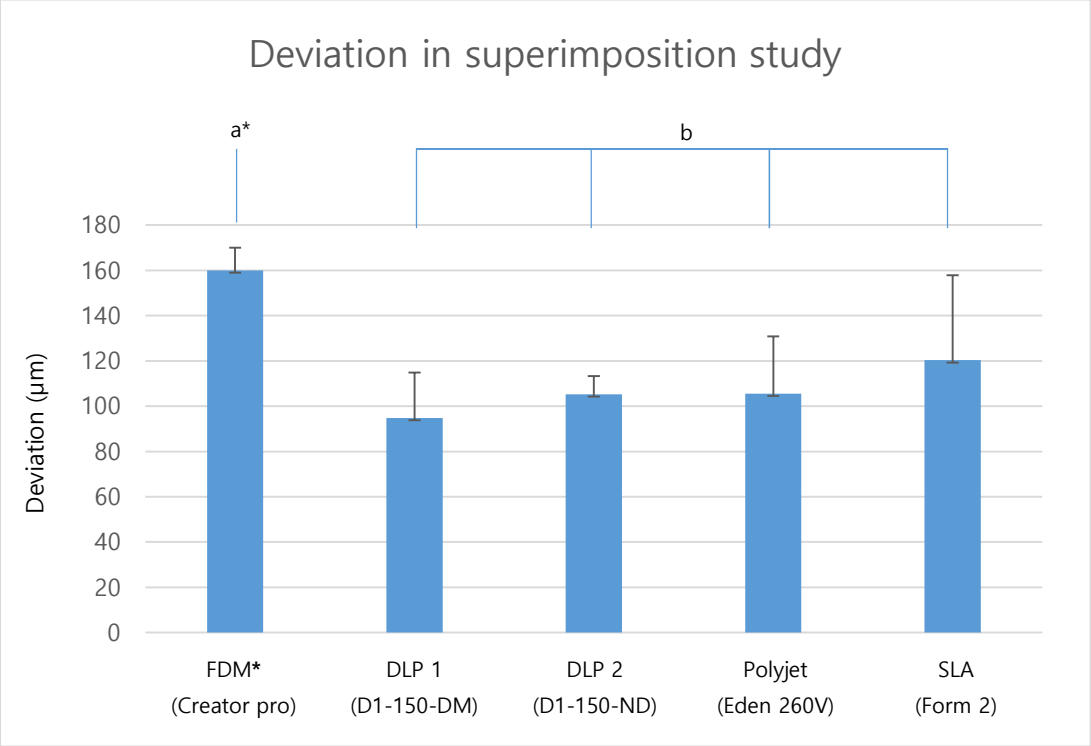

Fig. 6 FDM (Creator Pro) showed the highest mean deviation among the experimental groups ($p<0.05$*) and there were no significant differences among the other 4 groups. (unit: µm)

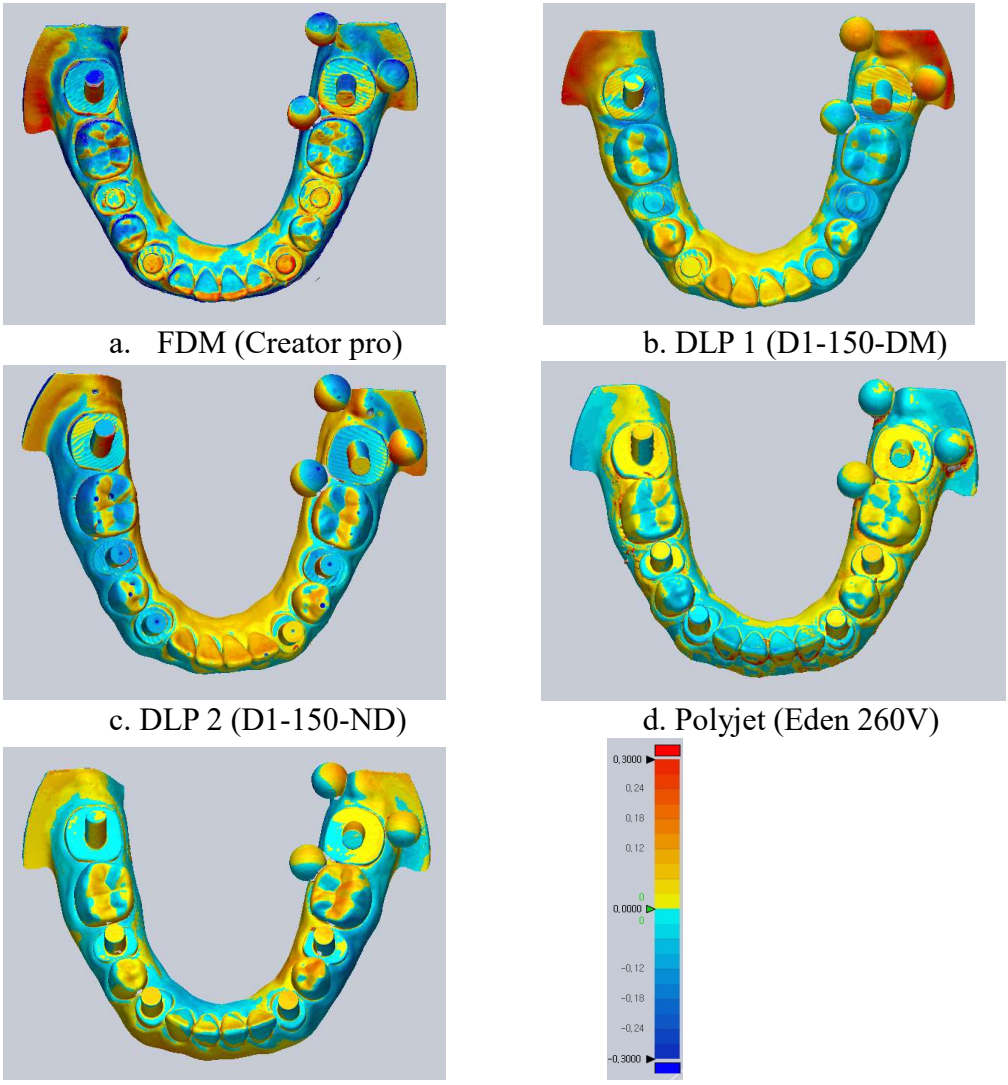

a. FDM (Creator pro) b. DLP 1 (D1-150-DM)

c. DLP 2 (D1-150-ND) d. Polyjet (Eden 260V)

e. SLA (Form 2) f.

Fig. 7 Color difference maps between the reference CAD data and FDM (Creator Pro) (a), DLP 1 (D1-150-DM) (b), DLP 2 (D1-150-ND) (c), Polyjet (Eden 260V) (d) and SLA (Form 2) (e). The map was set from -300 μm to 300 μm (f).

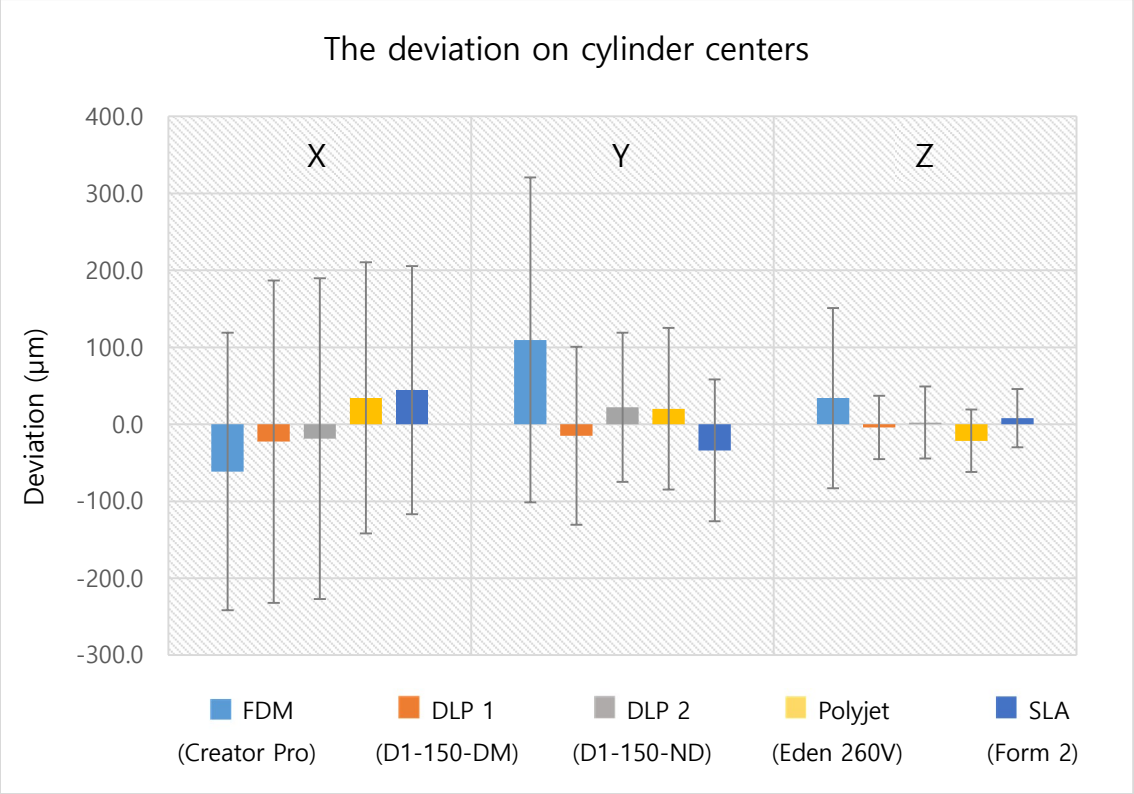

Fig. 8 The mean deviations in X-, Y-, and Z- coordinate of the cylinder top centers among 3D-printed models. (unit: μm)

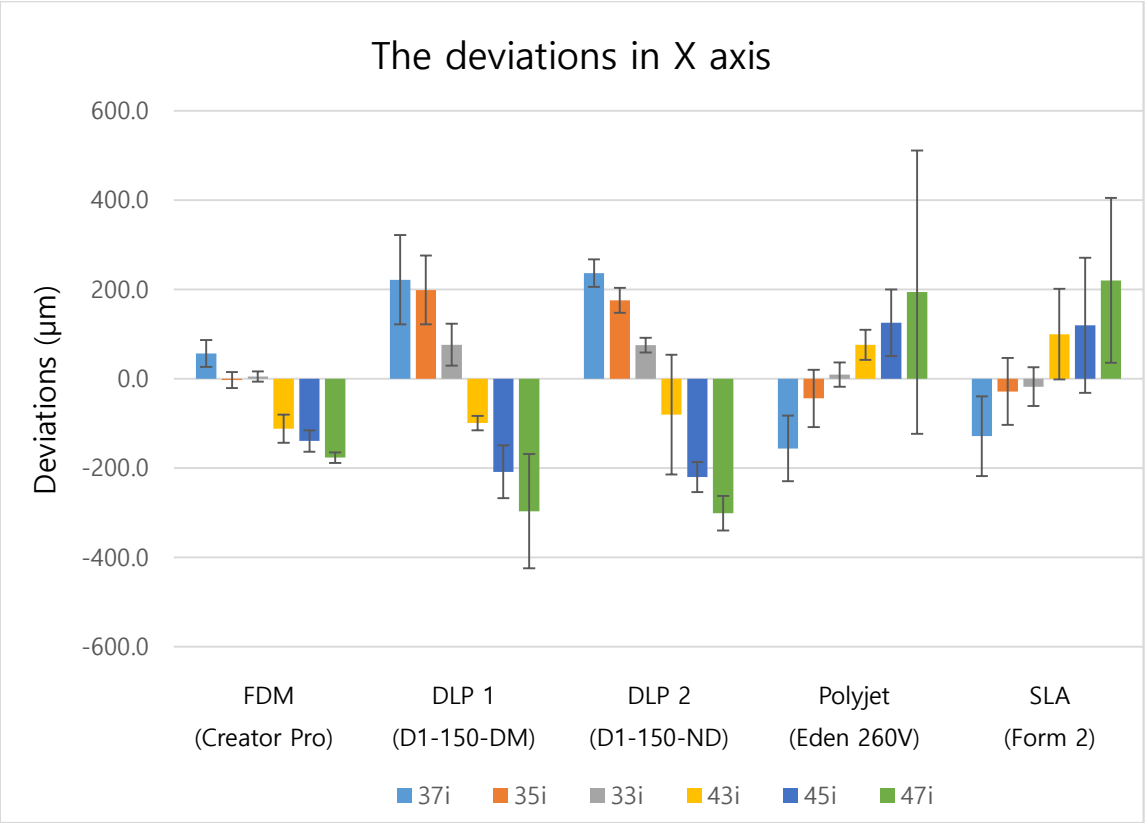

Fig. 9 The deviations in X axis of the 3D printers. (unit: μm)

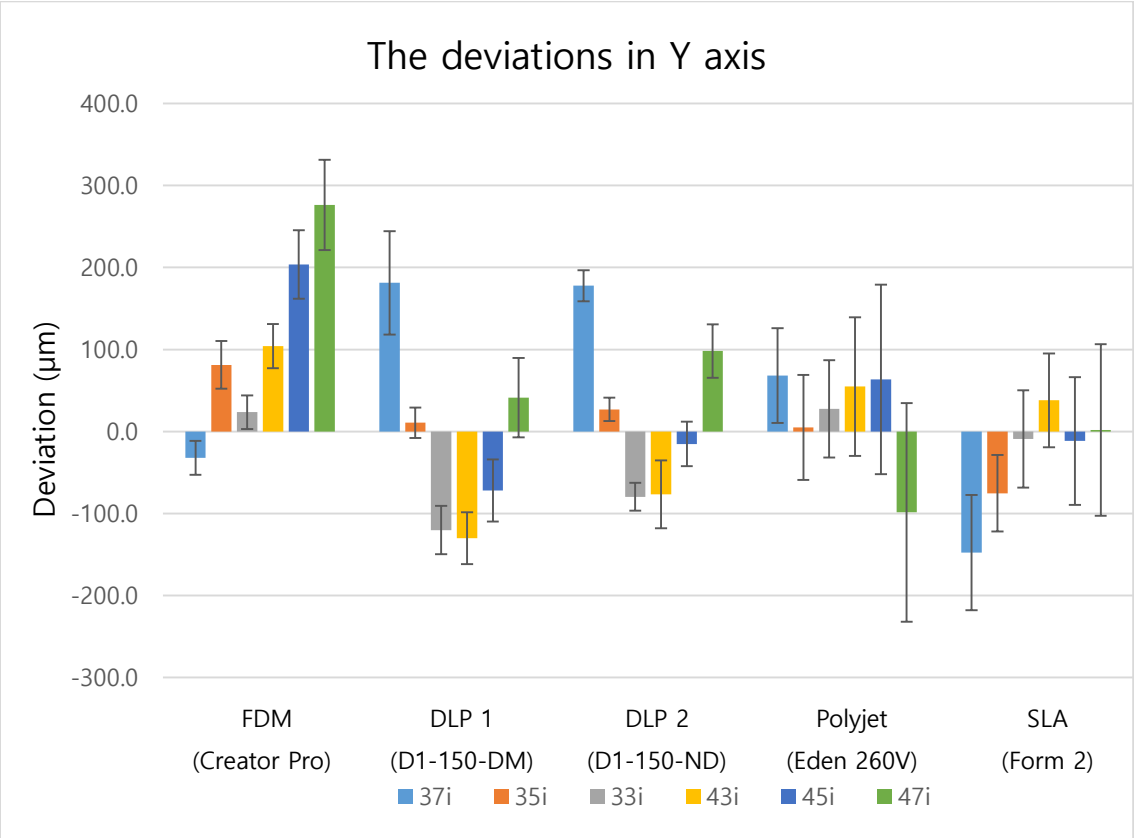

Fig. 10 The deviations in Y axis of the 3D printers. (unit: μm)

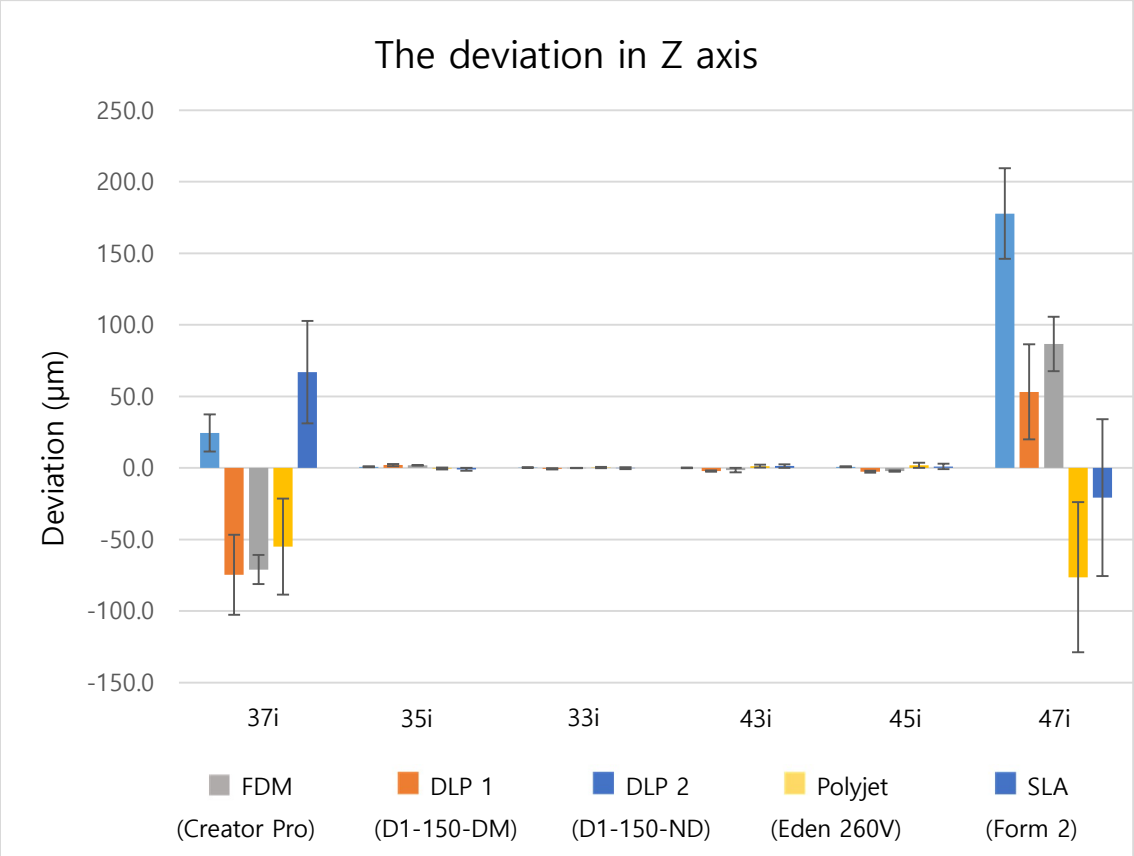

Fig. 11 The deviations in Z axis of the 3D printers. (unit: μm)

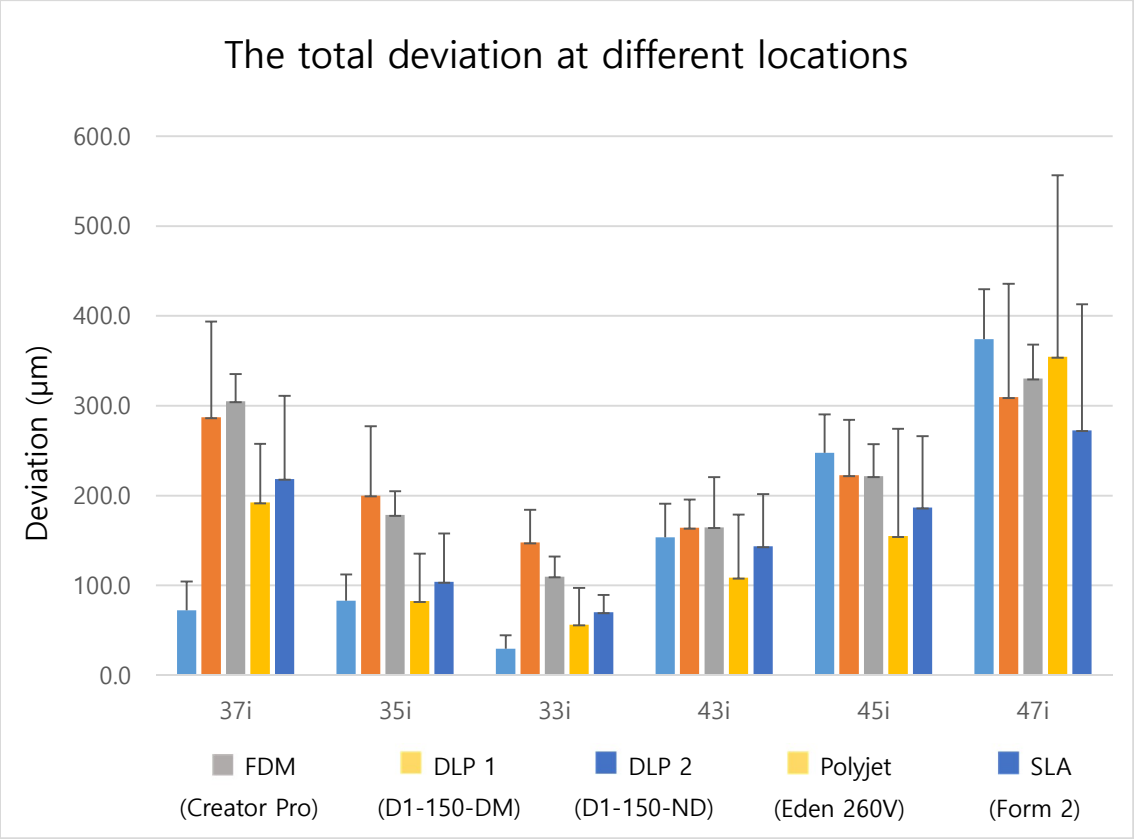

Fig. 12 The smallest deviations were detected at the #33i position and the largest deviations were detected at the #47i position in all groups. Positions farther from the #33i position showed increasing deviation sizes except for #35i, which showed larger deviations than #37i in FDM models. (unit: μm)

a1. FDM (Creator pro)

b1. DLP 1 (D1-150-DM)

c1. DLP 2 (D1-150-ND)

d1. Polyjet (Eden 260V)

e1. SLA (Form 2)

a2. FDM (Creator pro)

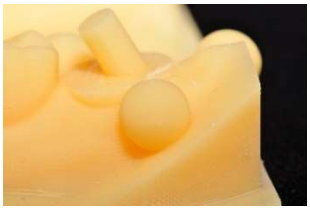

b2. DLP 1 (D1-150-DM)

c2. DLP 2 (D1-150-ND)

d2. Polyjet (Eden 260V)

e2. SLA (Form 2)

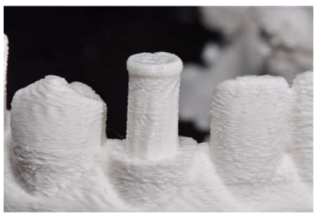

a3. FDM (Creator pro)

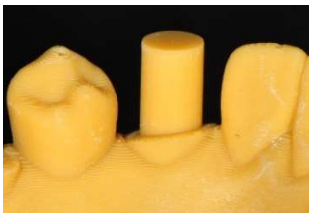

b3. DLP 1 (D1-150-DM)

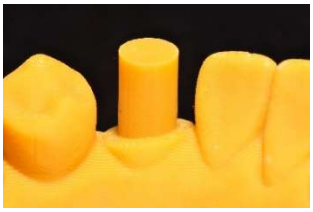

c3. DLP 2 (D1-150-ND)

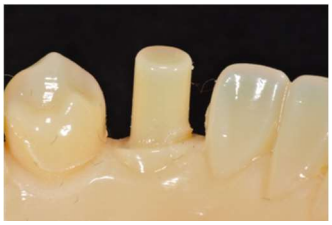

d3. Polyjet (Eden 260V)

e3. SLA (Form 2)

a4. FDM (Creator pro)

b4. DLP 1 (D1-150-DM)

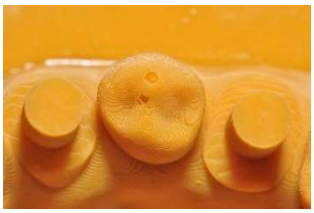

c4. DLP 2 (D1-150-ND)

d4. Polyjet (Eden 260V)

e4. SLA (Form 2)

Fig. 13 Photographed models of FDM (Creator Pro) (a) , DLP 1 (D1-150-DM) (b), DLP 2 (D1-150-ND) (c), Polyjet (Eden 260V) (d) and SLA (Form 2) (e) at various angles of mandibular anterior region (1), the buccal reference sphere (2), buccal view of canine cylinder (3) and top view of canine cylinder (4).

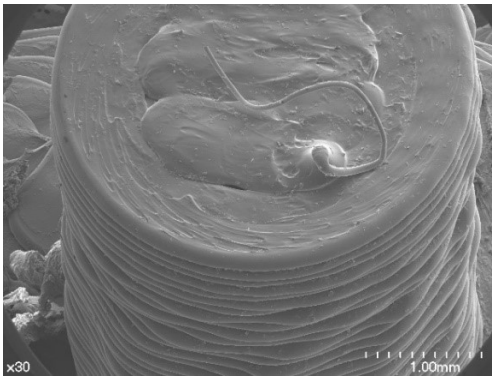

a. FDM (Creator Pro)

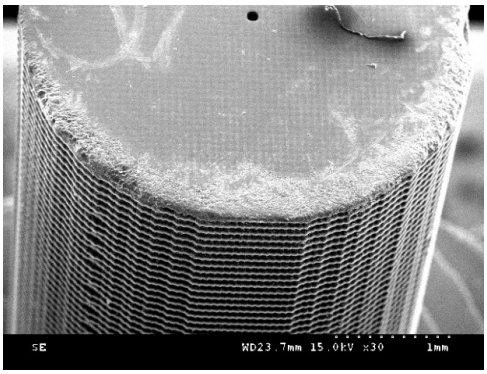

b. DLP 1 (D1-150-DM)

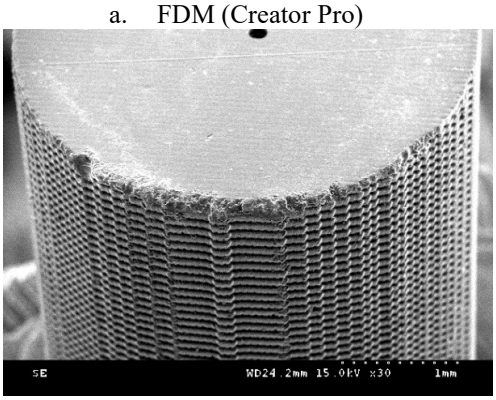

c. DLP 2 (D1-150-ND)

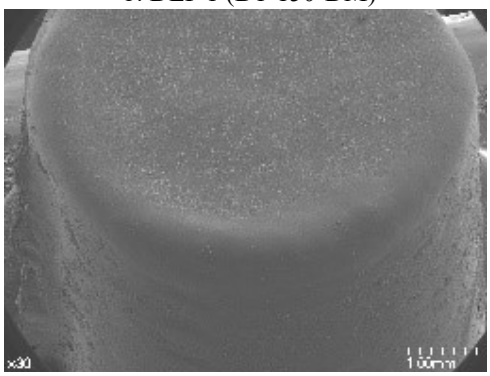

d. Polyjet (Eden 260V)

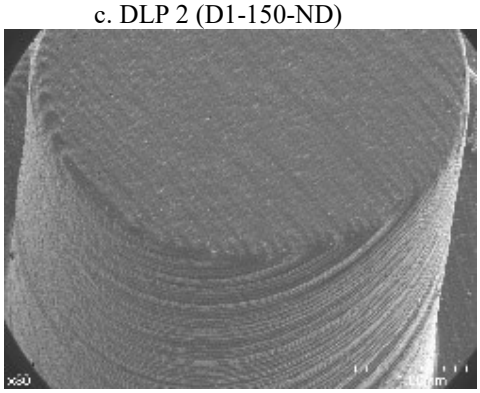

e. SLA (Form 2)

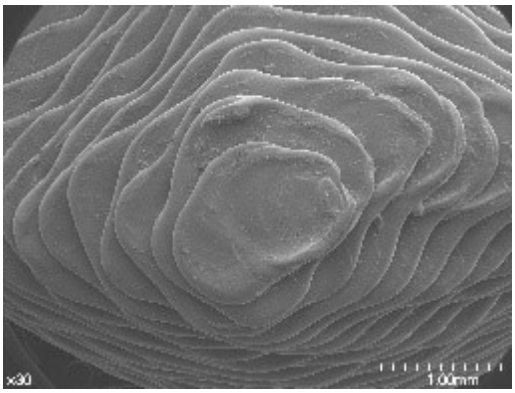

f. FDM (Creator Pro)

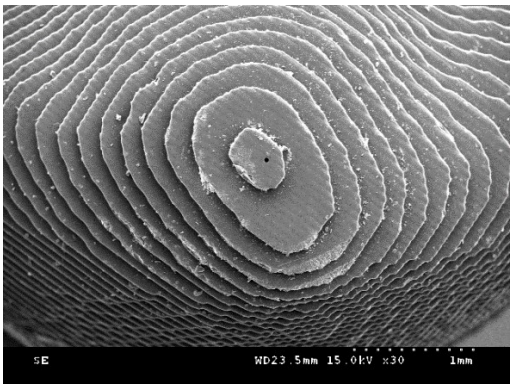

g. DLP 1 (D1-150-DM)

h. DLP 2 (D1-150-ND)

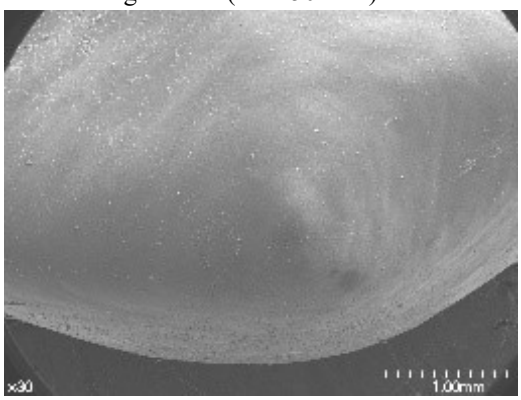

i. Polyjet (Eden 260V)

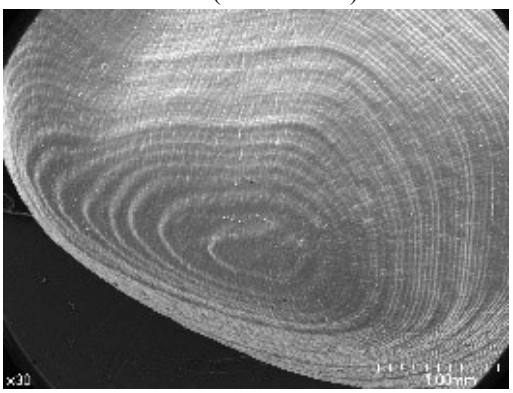

j. SLA (Form 2)

Fig. 14 SEM images with a magnification ratio of 30. The cylinder tops of FDM (Creator Pro) (a), DLP 1 (D1-150-DM) (b), DLP 2 (D1-150-ND) (c), Polyjet (Eden 260V) (d), SLA (Form 2) (e) and the premolar cusps of FDM (Creator Pro) (f), DLP 1 (D1-150-DM) (g), DLP 2 (D1-150-ND) (h), Polyjet (Eden 260V) (i), SLA (Form 2) (j).

Tables

Table 1 Specifications of experimental 3D printing groups

Group	Printer Name	Printing Scheme	Printer manufacturer	Materials	Material manufacturer
FDM	Creator Pro	FDM	Flashforge	Polylactic acid	Colorfabb
DLP 1	D1-150	DLP	Veltz3D	DM-1	Aekyung
DLP 2	D1-150	DLP	Veltz3D	Model	Nextdent
Polyjet	Objet Eden 260V	Polyjet	Stratasys	VeroDent(MED670)	Stratasys
SLA	Form 2	SLA	Formlabs	Gray	Formlabs

Table 2 Mean deviations of experimental 3D printers in superimposition study (unit: μm)

Printer	FDM (Creator pro)	DLP 1 (D1-150-DM)	DLP 2 (D1-150-ND)	Polyjet (Eden 260V)	SLA (Form 2)
Mean(SD)	160.0(10.0)^{a*}	94.7(20.2)^{b}	105.2(8.1)^{b}	105.5(25.4)^{b}	120.3(37.5)^{b}

$p<0.05$, FDM showed significantly more deviations than the other four groups.*

Table 3 The mean deviations in X, Y, Z coordinate of the cylinder centers among 3D-printed models (unit: μm)

Axis	FDM (Creator pro)	DLP 1 (D1-150-DM)	DLP 2 (D1-150-ND)	Polyjet (Eden 260V)	SLA (Form 2)
X	-61.3(180.4)^{a}	-22.5(209.4)^{a}	-18.8(208.4)^{a}	34.3(176.0)^{b}	44.4(161.1)^{b}
Y	109.5(211.0)^{c}	-14.8(115.6)^{a}	21.9(96.9)^{b}	20.1(105.0)^{b}	-34.0(92.1)^{a}
Z	34.0(117.2)^{d}	-4.2(41.2)^{b}	2.3(46.8)^{bc}	-21.4(40.6)^{a}	7.8(37.7)^{c}

The superscript letters represent significantly different subgroups of printers ($p<0.05$) in each axis. Subgroup 'a' had the lowest value and the next significantly different subgroup had the next alphabet.

Table 4 The deviations in X, Y, Z axes at different cylinder locations (unit: μm)

Axis	Location	FDM (Creator pro)	DLP 1 (D1-150-DM)	DLP 2 (D1-150-ND)	Polyjet (Eden 260V)	SLA (Form 2)
X	37i	56.6(29.9)^{d}	221.9(99.8)^{d}	236.7(31.1)^{d}	-155.9(73.5)^{a}	-128.5(89.0)^{a}
	35i	-2.7(17.9)^{c}	199.0(77.1)^{d}	175.8(28.0)^{d}	-43.8(64.3)^{ab}	-28.2(74.7)^{ab}
	33i	5.3(11.3)^{c}	76.4(47.1)^{c}	75.5(16.4)^{c}	9.6(27.3)^{abc}	-17.5(43.5)^{ab}
	43i	-111.7(31.6)^{b}	-99.0(16.0)^{b}	-80.0(134.0)^{b}	76.2(33.8)^{bc}	100.0(101.4)^{bc}
	45i	-139.1(23.9)^{b}	-208.3(59.1)^{a}	-219.8(33.6)^{a}	125.6(74.5)^{bc}	120.0(151.1)^{bc}
	47i	-176.4(12.0)^{a}	-296.4(127.7)^{a}	-301.0(39.0)^{a}	194.3(317.2)^{c}	220.3(184.5)^{c}
Y	37i	-32.0(20.6)^{a}	181.3(63.1)^{d}	177.7(18.9)^{e}	68.2(57.8)^{b}	-147.6(70.3)^{a}
	35i	81.2(29.1)^{c}	10.6(18.6)^{c}	26.9(14.1)^{c}	4.8(64.0)^{ab}	-75.3(46.7)^{ab}
	33i	23.6(20.5)^{b}	-120.2(29.6)^{ab}	-79.6(17.0)^{a}	27.7(59.3)^{b}	-9.2(59.3)^{bc}
	43i	104.2(27.0)^{c}	-129.9(31.6)^{a}	-76.5(41.4)^{a}	54.7(84.5)^{b}	38.1(57.2)^{c}
	45i	203.7(41.8)^{d}	-72.0(37.7)^{b}	-15.1(27.2)^{b}	63.6(115.5)^{b}	-11.6(77.8)^{bc}
	47i	276.4(55.1)^{e}	41.2(48.4)^{c}	98.1(32.7)^{d}	-98.7(133.4)^{a}	1.7(104.6)^{bc}
Z	37i	24.4(13.0)^{b}	-74.7(28.0)^{a}	-71.0(10.1)^{a}	-55.9(32.1)^{a}	66.9(35.8)^{b}
	35i	0.8(0.3)^{a}	1.9(0.8)^{b}	1.9(0.2)^{b}	-0.4(0.7)^{b}	-1.0(0.9)^{a}
	33i	0.3(0.2)^{a}	-0.5(0.4)^{b}	-0.1(0.1)^{b}	0.3(0.4)^{b}	-0.3(0.7)^{a}
	43i	0.0(0.3)^{a}	-2.2(0.4)^{b}	-1.5(1.6)^{b}	1.2(1.0)^{b}	1.3(1.3)^{a}
	45i	0.8(0.4)^{a}	-2.7(0.8)^{b}	-2.2(0.5)^{b}	1.8(1.8)^{b}	1.0(1.8)^{a}
	47i	177.7(31.7)^{c}	53.1(33.3)^{c}	86.6(19.0)^{c}	-76.5(52.5)^{a}	-20.8(54.8)^{a}

The superscript letters represent significantly different subgroups of locations ($p<0.05$) in each printer and in each axis. Subgroup 'a' had the lowest value and the next significantly different subgroup had the next alphabet.

Table 5 The total amount of linear deviation at the cylinders (unit: μm)

Location	FDM (Creator pro)	DLP 1 (D1-150-DM)	DLP 2 (D1-150-ND)	Polyjet (Eden 260V)	SLA (Form 2)
37i	72.4(32.0)^{ab}	287.1(106.5)^{bc}	305.1(30.3)^{d}	192.5(65.1)^{a}	218.6(92.5)^{cd}
35i	82.9(29.4)^{b}	200.1(77.1)^{ab}	178.6(26.5)^{bc}	82.8(52.8)^{a}	104.2(53.7)^{ab}
33i	29.6(15.1)^{a}	147.9(36.4)^{a}	109.9(22.4)^{a}	56.5(40.9)^{a}	70.2(19.3)^{a}
43i	153.8(37.3)^{c}	164.1(31.4)^{a}	164.8(55.8)^{b}	108.8(70.1)^{a}	143.7(57.9)^{abc}
45i	247.6(42.8)^{d}	222.7(61.9)^{abc}	221.6(35.6)^{c}	155.1(119.2)^{a}	186.7(79.6)^{bcd}
47i	374.3(55.6)^{e}	309.5(126.2)^{c}	330.3(28.0)^{d}	354.5(202.0)^{b}	272.8(140.4)^{d}

The superscript letters represent significantly different subgroups of locations ($p<0.05$) in each printer. Subgroup 'a' had the lowest value and the next significantly different subgroup had the next alphabet.

국문초록

다양한 3D 프린터로 제작한 치과 모형의 정확도 평가

서울대학교 대학원 치의과학과 치과보철학 전공
(지도교수 **허 성 주**)
전 진

연구목적

구강 스캐너로 광학 인상을 채득하는 기술과 CAD/CAM 을 이용하여 보철물을 제작하는 방법이 1980 년대 초에 소개되었다. 구강 스캐너의 발전과 사용 빈도의 증가로 종래의 인상 없이 악궁 정보를 디지털 데이터로 직접 획득하는 방법이 더 대중화되고 있다. 디지털 인상을 사용하면 간단한 경우에 물리적 모델 없이 보철물 제작이 가능하지만, 광범위한 수복 등 많은 경우에는 여전히 물리적 모델이 필요하다. 디지털 인상 데이터로 물리적인 모델을 만들기 위해 원판 혹은 블록을 깎는 밀링 과정이나 3D 프린팅 (rapid prototyping) 방법이 사용될 수 있다. 이 연구의 목적은 DLP (Digital Light Processing), FDM (Fused Deposition Modeling), SLA (Stereolithography), Polyjet (Photopolymer jetting)의 다양한 3D 프린터로 출력한 모형의 정확성과 재현성을 비교 평가하는 것이다.

연구 재료 및 방법

역설계 프로그램으로 하악 모델을 변형하여 기준 악궁 캐드 데이터를 제작하였다. 임플란트 스캔 바디를 재현하기 위해 하악 모델의 좌우 견치 (#33, #43), 좌우 제 2 소구치 (#35, #45), 좌우 제 2 대구치 (#37, #47)에 총 6 개의 기둥을 설계하였다. 식립 방향이 축에서 벗어난 임플란트 바디를 재현하기 위해 좌측 그리고 우측 제 2 대구치 기둥은 각각 근심 원심으로 30 도 기울여 디자인하였다. 좌측 제 2 대구치 주변으로 좌표 축을 설정하기 위한 기준 구를 3 개 추가 디자인하였다. 4 종의 3D 프린터 (FDM (Creator Pro), DLP (D1-150), Polyjet (Eden 260V), SLA (Form 2))와 5 종의 다른 재료를 이용하여 기준 캐드 디자인 파일을 각 그룹당 10 개씩 출력하였다. 출력된 모델은 모델 스캐너를

이용하여 스캔하고 스캔한 파일을 원본 디자인 파일과 정합하였다. 중첩연구에서는 전체적인 평균 변이를 분석하였고, 좌표 연구에서는 각각 기둥의 위치에서 X, Y, Z 축의 변이량과 선형 변이량를 분석하였다. 변이를 가시화하기 위해 색차이 지도와 사진, SEM 상에서 표면을 분석하였다.

결과

중첩연구에서 FDM 모델이 통계적으로 의미 있는 큰 변이를 보였고 ($p<0.05$) 다른 프린터 그룹에서는 통계적으로 의미 있는 차이가 없었다. X 축에서 FDM 과 DLP 는 좌측 제 2 대구치에서 가장 많은 변이를 보였으며 오른쪽으로 갈수록 변이량이 줄어들고 반대로 SLA 와 Polyjet 은 좌측 제 2 대구치에서 가장 큰 음의 변이를 보였으며 오른쪽으로 갈수록 변이 값이 커졌다 ($p<0.05$). Y 축에서 FDM 은 중간에서 오른쪽으로 갈수록 전방부 변이를 보였으며, DLP 는 전치부에서는 후방으로, 구치부에서는 전방으로 변이를 보였다. Z 축에서 모든 프린터가 견치와 제 2 소구치 부위에서 변이가 적었으나 제 2 대구치에서는 변이가 존재하였다 ($p<0.05$). 모든 프린터에서 전체 변이량은 좌측 견치가 가장 적었고, 이 부위에서 멀어질수록 점점 더 커졌다 ($p<0.05$).

결론

중첩연구에서 FDM 이 가장 많은 체적 변이를 보였다. 좌표 연구에서 협설 기준으로 FDM 과 DLP 는 협측 방향으로 팽창하였고 Polyjet 과 SLA 는 설측으로 수축하였다. 전후 기준으로 FDM 은 전체적으로 전방 변이를 보였으며 DLP 는 구치 부에서는 전방 변이, 전치부에서는 후방 변이를 보였다. 모든 프린터에서 전치와 견치부에서 수직 변이량은 많지 않았으나 구치부에서는 유의한 수직 변이가 관찰되었다. 위치에 따른 전체 변이량은 모든 프린터에서 견치부위에서 가장 낮았으며 견치에서 멀어질수록 더 커졌다.

주요어: 3D 프린팅, 정확도, 적층 가공, 치과 모형, 쾌속 조형

학번: 2013-31204